The Influence of Core Shape and Material Nonlinearities to Corner Losses of Inductive Element

Magdalena Puskarczyk[1], Brice Jamieson[1], Wojciech Jurczak[1]
[1] ABB Corporate Research Centre, Kraków, Poland

Abstract: The effects of sharp corners on the flux distribution in a ferromagnetic core are modeled using COMSOL Multiphysics to determine the time-domain flux density for an applied field which is uniform in the non-corner section of the core. The frequency spectrum of the flux distribution is calculated for a series of points through the corner and the effects of harmonic frequencies on the flux and loss profiles are analyzed. The contribution of higher-order harmonics is presented and shown to contribute up to 3.8% of the total loss in the areas of the core where the flux enhancement is highest. Flux reduction is also considered in the outer edges of the core and shown to be dependent on harmonic frequencies in the flux profile.

Keywords: choke, transformer, flux distortion

1. Introduction

Soft ferromagnetic cores are a key part in the conversion of power from a source at one level of current and voltage to a load at another level. These components are found in distribution transformers serving national power grids, in mobile phone chargers, and at all power levels in between. Many of the cores used for these systems are E-I shaped or pot cores and many are sold as commodity components in standard shapes and sizes which are selected for the application. These losses are usually determined from loss equations for uniform magnetic materials under specified excitation conditions, provided by the core manufacturer. Sharp corners in the magnetic core, however, can cause flux enhancement effects [1] leading to a non-uniform flux profile. These enhancement effects cause variations in the core magnetization leading to higher losses than in a bulk material. As well, the enhancement effect is not uniform and varies with position in the core and frequency of the AC flux. Determining more precisely the effect of core shape on losses in such an application can provide an important insight into designing more electrically-efficient and cost-efficient cores with better high-frequency properties.

2. Use of COMSOL Multiphysics

2.1 Mathematical description

Although losses in the core are typically given as datasheet parameters (see Figure 1), there are known models for loss in a material. The most common of these is the Steinmetz equation, describing the magnetization of a ferromagnetic core under the influence of an AC magnetic field. This is a general-form equation and can be used to model various types of ferromagnetic loss, taking the general form in (1) where K, n, and a are experimentally-determined material constants, f is the excitation frequency, and B is the flux in the core.

$$P = Kf^{n}B^{a} \quad \textbf{(1)}$$

For hysteresis loss, the form of the Steinmetz equation in (2) is used to determine P_H, the total hysteresis loss of a core per unit volume during one magnetization cycle.

$$P_H = K_H f B_{\max}^{\alpha} \quad \textbf{(2)}$$

For eddy-current loss, the loss associated by currents induced the material opposing the flux produced by the winding, the form of the Steinmetz equation in (3)

$$P_E = K_E f^2 B_{\max}^2 \quad \textbf{(3)}$$

For a core provided by the manufacturer, a modified Steinmetz-form equation for total core loss is often provided. This equation is usually given for standard operating frequencies based on experimentally obtained data, shown in (4).

$$P_{fe} = K_{fe} B_{\max}^{\beta} A_c l_m \quad \textbf{(4)}$$

In the above equation, A_c and l_m are the cross-sectional area and path length of the core respectively, while β and K_{fe} are experimentally determined and typically provided in the form of a chart from which the total power loss can be determined, shown for MPP material in (1).

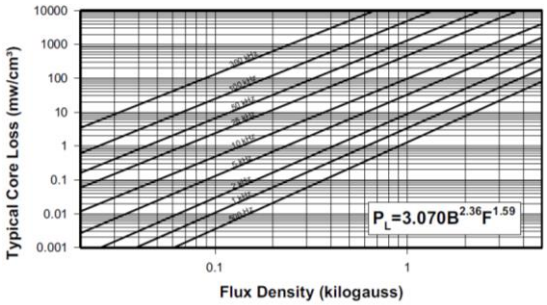

Figure 1 Manufacturer-provided total power loss graph for MPP powder ferrite material.

As expected, these loss calculations are highly specific to the core and application and a method to accurately model variation in these parameters would be a valuable tool for designers.

2.2 Simulation setup description

The goal of the simulation was to investigate nonlinear distributions of magnetic flux density in a ferromagnetic core. The magnetic device under investigation consists of a square-shaped core and two coils. Using COMSOL 4.3a, the AC/DC Module was utilized with the Magnetic Field and Electrical Circuit interfaces to describe the model.

The magnetic device is represented as finite element model, but the coil is powered by signal source represented by equations provided by the Electrical Circuit interface (Figure 2).

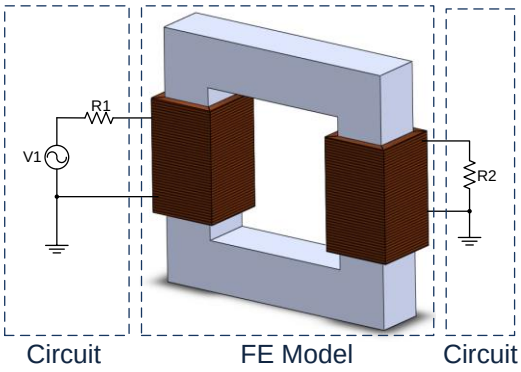

Figure 2 Two coils wound around a core, modeled as a finite element model, while the load and power source are represented as equivalent electrical circuit.

In the presented model the finite element (FE) model takes into account the non-linearity of the magnetic materials and is suitable for a deep study of uneven saturation phenomena of the core. To observe time-domain waveforms of B and H a grid of testing points was defined in one corner region of the core.

The material properties of the real choke were assigned to individual geometric domains of the model. The core is made of Molypermalloy Powder (MPP) 550µ pressed-powder material and the permeability is described by the hysteresis curve supplied by the manufacturer [2]. From this, the nonlinear knee region of the curve begins at approximately 0.6 T before saturating at 0.8 T. MPP cores are characterized by low hysteresis losses and high resistivity [2], thus the core material was described as isotropic but nonlinear which is a good approximation of the real powder core material properties.

The unstructured tetrahedral mesh was applied to all domains of the FE part of the model. The mesh size and distribution are carefully controlled, especially in regions where we can expect saturation or other nonlinear changes in flux density with increasing magnetization.

The Time Dependent analysis with a time step of 10^{-4}s was applied to the model. As the FE model is described by equations provided by the Magnetic Field interface and the constraints are defined by the Electrical Circuit interface, a fully coupled solution approach is needed. In this approach the equations of both interfaces are solved simultaneously.

For solving nonlinear models a common problem is to obtain a convergent solution. Here, to avoid trouble with convergence, the time step was decreased in the time dependent solver. Additionally, the tolerance factor was decreased and the maximum number of iterations increased compared to the default solver settings [3]. All of these operations increase the stability of the process of solving nonlinear problems.

2.3 Multi-turn Coil Domain

The function of coils in the model is to magnetize the core to a mean flux density of 0.56 T, which is just below the point where the material becomes nonlinear. Two coils were modeled using the COMSOL Multi Turn Coil Domain (MTCD) feature. Each coil was drawn as a solid domain and then the MTCD feature was applied for the whole volume of the coil.

MTCD is a way of applying effective current density vectors (Figure 3) to the domains, which will on average give the same current density as in a "real" coil consisting of the same number of turns as defined in MTCD. The MTCD is applied to a solid domain which in a real device contains both the coil and the insulator (e.g. air) which is between the coil windings. In a coil described by MTCD the distribution of the wires in space (e.g. how many layers in the coil) is neither considered nor described.

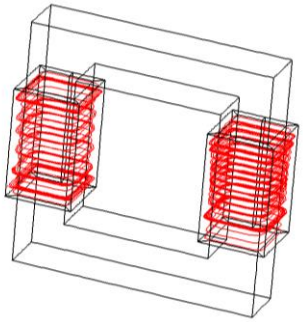

Figure 3 Coil direction vectors drawn as streamlines.

The described simulation setup cannot be used to observe physical phenomena affecting the windings like the proximity effect but only the core response for an applied magnetic field. In this analysis we will restrict ourselves to only the magnetic effects inside the core and because we assume the wires in the coils are evenly distributed, the MTCD feature is determined to be a good enough approximation of the real solenoid which magnetizes the core.

2.4 Use of the Electrical Circuit Interface

The primary winding of the model is powered from an electrical circuit coupled with the 3D FE model through the Multi Turn Coil Domain feature (Figure 2). In the simulation setup the first coil is powered by a 7 V (amplitude) 50 Hz sine voltage source while the second coil is shorted with a large resistor, R2, in order to approximate open circuit conditions. Using the voltage source is an easy way to ensure the desired amplitude and phase of the power source.

For numerical stabilization a small resistor R1 (0.1 Ω) was connected in series with the coil. The resistor represents the resistance of the primary windings. The resistor R2 (1000 Ω) represents the open circuit condition for the coil L2. This representation of the open circuit condition is used because it makes the model more versatile – a resistor can be easily replaced by any other type of load.

3. Simulation results

The magnetic flux density in the selected corner region of the core is presented in Figure 4.

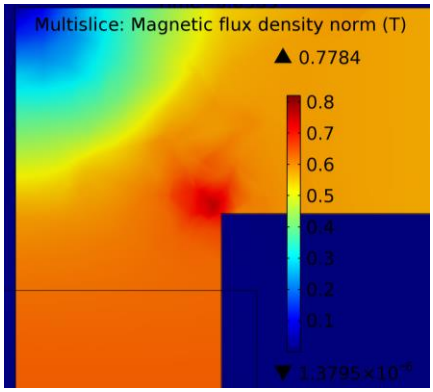

Figure 4 Magnetic flux density around a right-angled corner of the choke.

As shown in Figure 4, the magnetic flux is enhanced around the inner square corners and reduced significantly in the outer square corners. The largest concentration of magnetic flux can be seen in this inner corner region, with a peak amplitude of above 0.6 T, indicating that the core is being driven into the nonlinear region of the hysteresis curve.

Figure 5 shows a single layer of the grid of points used to measure the field. The complete grid consists of 175 elements, distributed around the corner in five layers (35 points per each layer) [4]. As an output of the simulation the time-domain waveforms of each point on the grid were stored.

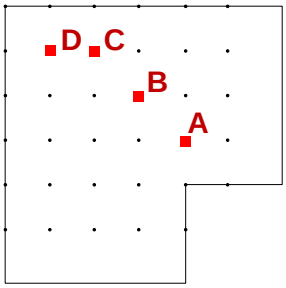

Figure 5 A grid of testing points (single layer localized in the middle of the core). Four exemplary points, A, B, C and D, are marked in red.

Figure 6 and Figure 7 show the time waveforms of the x components of magnetic flux density, B, and magnetic field, H, for the exemplary points, A, B, C and D placed inside the core to show areas of expected enhanced flux, uniform flux, pseudo-uniform flux, and reduced flux respectively. These behaviours were seen in the analysis roughly as expected.

As seen in the magnetic field and magnetic flux density for other points (not pictured), the waveforms make an almost-symmetrical pattern about a diagonal in the corner, due to the magnetic isotropy of the core material. Notably, while there is a visible waveform distortion for the inner corner region, as expected, there is also a similar distortion in the outer core region, however instead of a flux enhancement there is a flux reduction, due to the nature of flux lines to find the path of lowest reluctance, in this case through the shortest distance. For flux in the outer edge of the core the path length and, by extension, the reluctance would increase leading to an undesirable path. Therefore more flux is found in the inner corner as observed.

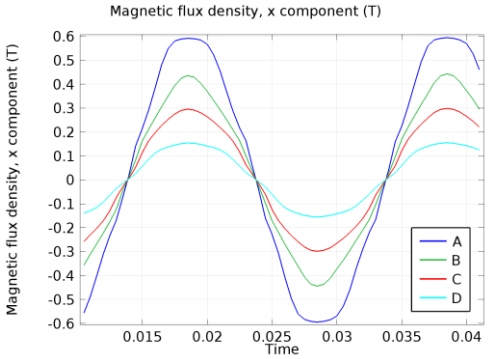

Figure 6 Time waveforms of x-component of magnetic flux density (Bx) in four exemplary points, A, B, C and D, inside the core.

Figure 8 presents the different hysteresis curves described by Bx and Hx for exemplary points A, B, C and D. Note, the first knee point at +/-100 A/m is, in this analysis, due to the hysteresis data used in the simulation and is not due to nonlinearities in the flux.

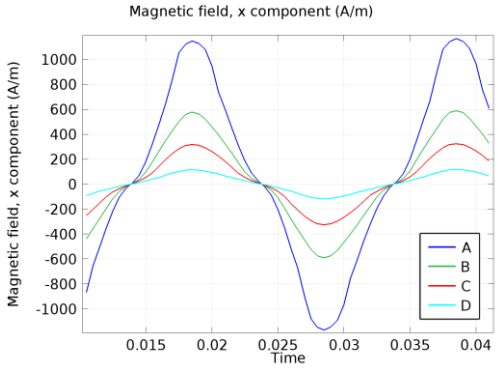

Figure 7 Time waveforms of x-component of magnetic field (Hx) in four exemplary points, A, B, C and D, inside the core.

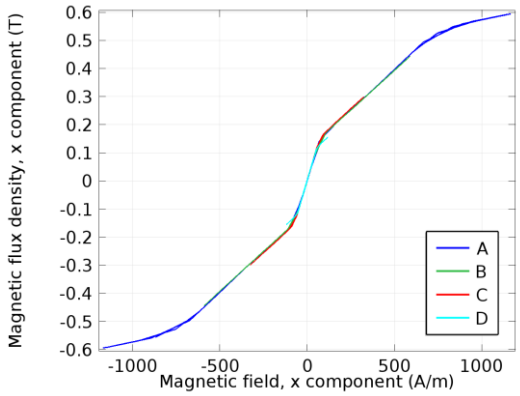

Figure 8 Hysteresis curves for selected points inside the core.

During a typical traversal of the hysteresis loop (one AC voltage period) the permeability of each point inside the core changes according to some local hysteresis curve limited by different maximal values of B. For a fixed amplitude of the power source, the magnetic flux density at some points inside the core never enters the nonlinear region while the other points are driven well past the nonlinear region and into saturation. Since saturation and nonlinearity can be easily observed in the shape of the flux waveform, it is helpful to visualize this in the frequency domain. Figure 9 shows the frequency spectrum of Bx at each point A, B, C and D.

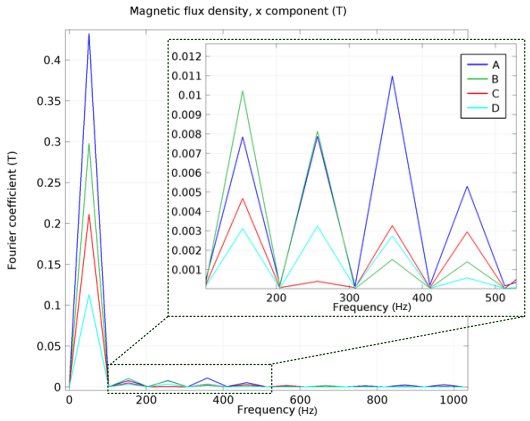

Figure 9 Fourier spectrum of the x component of magnetic flux density for points A, B, C, D.

In Figure 9, it can be observed that the magnetic flux waveforms are distorted at every testing point, not only in the region where the material is saturated but also in regions where the amplitude is comparatively low. What is more, at each point the higher harmonic spectrum is different: some harmonics are high while others may be low or not occurring at all. At point B, for example, the harmonics generally behave as expected, with increasing order harmonics having a lower magnitude, however notably the seventh harmonic is of approximately the same magnitude as the ninth, both of which are quite lower than the fifth. In point C, however the fifth harmonic almost vanishes and in point A, most notably, the seventh harmonic is larger than any of the other higher-order harmonics.

4. Conclusions

Fourier analysis of the magnetic flux density reveals a very important feature: although the coil, which magnetizes the core, is powered by a sinusoidal signal the magnetic flux in the corner region of the core is definitely not sinusoidal. As well, even though the applied field was designed to not push the core into the nonlinear region, the enhancement effects caused areas of the core to be driven well into this region. Because of these flux distribution nonlinearities higher-order harmonics (order ≥ 3) are present in the flux waveform which cause additional losses. Thus the losses in corner region are higher than calculated according to modified Steinmetz equation for this material (equation (1)), because this equation assumes there will be only a single (fundamental) harmonic of the magnetizing field in the core. A loss spectrum for points A, B, C and D is shown in Figure 10, illustrating the contribution of these higher-order peaks, particularly the third and seventh as well as the significant contribution of these higher-order harmonics in point A, where the maximum amount of field distortion is observed.

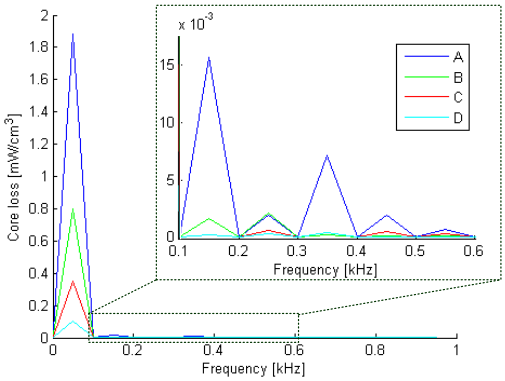

Figure 10 Loss spectrum for points A, B, C and D.

To analyze the importance of higher harmonic losses at each point of the test grid, the losses caused in a point by harmonics of order higher than the fundamental were calculated. These were shown as a percentage of the average total core loss at each point. The value of higher-order harmonic losses for each point was taken, averaged across the three centre layers and compared to the total loss for the core distributed evenly across all points, as would be expected in the uniform material model. The reason for averaging across three centre layers is because the model is relatively independent in the z-direction (into the page) and by averaging the centre three layers (those inside the core and not lying on the surface) we are able to reduce the graph to a roughly 2D approximation of loss and thus a simplified comparison of the effects of flux path on total loss. The value in such an analysis is that it shows the impact of higher-order harmonics on total core loss as a function of position, as well as showing the deviation from expected loss values. Figure 11 depicts this percentage ratio, showing a higher influence of harmonic losses in the corner regions. Losses were calculated according to manufacturer data.

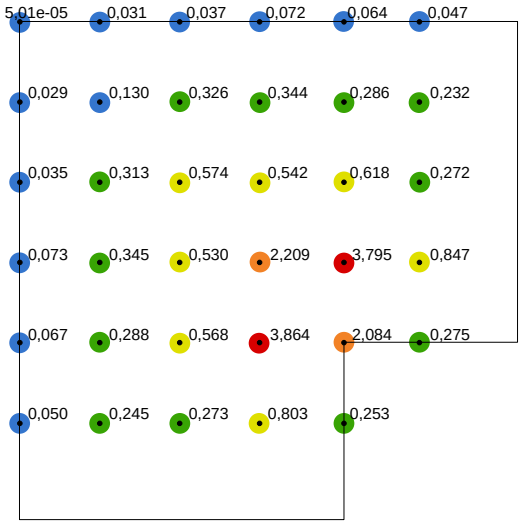

Figure 11 Percentage ratio of higher harmonics losses presented against a heat map of average point losses for the test grid. (Mean value of the three inner layers of test points shown).

Analysis of Figure 11 reveals that in the inner region of the core the higher harmonic losses are up to 3.8% of the fundamental harmonic losses. For small power cores this value is relatively small and can be neglected but for high power applications these losses are quite significant, particularly when efficiency of $\geq$ 95% is desirable. In the outer corner region the magnetic flux density is also highly distorted, although these distortions do not cause the same overall - high losses as in the inner core region. Additionally, the effects of higher-order harmonics are shown to not behave uniformly with distance from the centre diagonal (considering points radiating along x and y axes from a diagonal point). Rather, it is just off the central diagonal where the maximum influence of higher-order harmonics is observed. The influence of harmonics also is larger in almost all non-edge points than it is at a point in the core with a "uniform" field, using the second column of points as an example where the "uniform" field point has a higher-order harmonic contribution of 0.245, compared to a maximum of 0.345 in the same column. From this, we can expect that the non-uniform flux profile in the core contributes to increased losses as well as increased higher-order harmonics in the corner. Finally, this analysis shows that the losses due to harmonics are significant in the corner region of a core and are not uniform and scalable as they would be in a bulk material.

5. References

1. Hernández, J. M. Cañedo, J. C. Olivares-Galván and P. S. Georgilakis, Electromagnetic Analysis and Comparison of Conventional-Wound Cores and Octagonal-Wound Cores of Distribution Transformers, *Materials Science Forum* **Vol. 670** pp 477-486(2011)
2. *Powder Cores Catalog*, Magnetics Inc. available online: http://www.mag-inc.com/products/powder-cores/mpp-cores/mpp-material-curves
3. http://www.comsol.com/support/knowledgebase/1127/
4. F. Brailsford, V. R. Mazza, The alternating magnetic flux distribution in right-angled corners of transformer laminations. An Experimental Investigation, *Proceedings of the IEE Part A: Power Engineering* **Vol. 109** pp 173-180(1962)